Journal of Thermal Analysis and Calorimetry, Vol. 70 (2002) 703–711

SELF-ORDERING PROCESS OF PHENANTHRENE POLYESTERS OBSERVED BY THE SIMULTANEOUS DSC-XRD METHOD

H. Yoshida[1*], *M. Yang*[1], *K. Masaka*[2], *Y. Houshito*[2], *K. Mashiko*[2] *and S. Nakamura*[2]

[1]Graduate School of Engineering, Tokyo Metropolitan University, Hachiohji, Tokyo 192-0397, Japan
[2]Department of Applied Chemistry, Kanagawa University, Kanagawa-ku, Yokohama 221-8686, Japan

Abstract

Phase transition behavior of polyesters derived from 2,7-phenanthrene dicarbonic acid diethylester and alkanediols with even methylene carbon number was investigated by the simultaneous DSC-XRD method. The smectic A phase was observed on cooling from the molten state. The transition entropy from the isotropic state to the smectic A phase was about 9.0 J mol^{-1} K^{-1}, which depended on the methylene carbon number. The linear expansion coefficients, based on the (001) spacing of the crystalline phase at room temperature, were $1.3\cdot10^{-4}$ K^{-1} (crystalline phase), $5.7\cdot10^{-4}$ K^{-1} (crystallization region), $1.7\cdot10^{-3}$ K^{-1} (smectic A phase) during cooling, and $1.5\cdot10^{-4}$ K^{-1} (crystalline phase), and $1.0\cdot10^{-3}$ K^{-1} (melting region) on heating.

Keywords: DSC-XRD, liquid crystal, phenanthrene, polyester, thermal expansion

Introduction

The thermotropic polyesters based on 2,7-phenanthrene dicarbonic acid diethylester and alkanediols assume the smectic liquid crystalline phase above their melting temperatures due to the intermolecular interaction between phenanthrene moieties [1, 2]. Phenanthrene moieties as a mesogenic unit are connected by alkyl chain in the main chain of phenanthrene polyester; PPE. These polyesters having phenanthrene moieties in the main chain exhibit the odd-even effect of methylene carbon number (*n*) on the phase transition temperature and the transition enthalpy of PPE. The transition temperature of PPEs with even *n* number is higher than that of PPEs with odd *n* number [1, 2].

Poly(oxyheptamethyleneoxy-2,7-phenanthrenedicarbonyl) (PPE*n*7) demonstrates the smectic A and C phases on cooling by the simultaneous DSC-XRD [3]. At the transition from the smectic A to the smectic C phases on cooling, the (001) spacing of PPE*n*7 changed discontinuously from 1.9 to 1.8 nm, however, the linear expansion coefficients

---

[*] Author for correspondence: E-mail: yoshida-hirohisa@c.metro-u.ac.jp

1418–2874/2002/ $ 5.00

Akadémiai Kiadó, Budapest
Kluwer Academic Publishers, Dordrecht

in both smectic A and C phases were the same [3]. The same linear expansion coefficient indicates that the smectic phase exists on heating for PPE*n*7 [3]. Liquid crystalline phase of polymer is often observed on cooling, while it is hard to observe on heating due to the narrow temperature range [4–6]. The linear expansion measurement is powerful tool to determine the phase which exists in the narrow temperature region between the melting and the isotropic transitions. The temperature range of the smectic phase observed on cooling is considerably narrow for PPEs with even *n* number comparing with that for PPEs with odd *n* number. In this study, the phase transition and linear expansion of PPEs with even *n* number were determined by the simultaneous DSC-XRD method.

Experimental

Phenanthrene polyesters (PPE) (Scheme 1) were prepared by polycondensation of 2,7-phenanthrene dicarbonic acid diethylester and corresponding alkanediols. The PPE samples were purified by the precipitation method from *m*-cresol/*o*-chlorophenol solution to a large amount of methanol. The intrinsic viscosity [η] evaluated at 30°C using the mixed solvent of phenol and 1,1,2,2,-tetrachloroethane (6:4) were 0.34, 0.34 and 0.51 dL g^{-1} for PPE*n*6, PPE*n*7 and PPE*n*8, respectively. The PPE powder was pressed into a disk with 0.5 mm thickness. The disk of PPEs with about 3 mg was sealed by aluminum foil and was clamped in the aluminum pan for the DSC-XRD measurement.

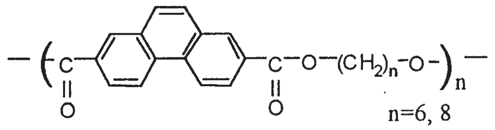

Scheme 1

DSC measurements were carried out by Seiko DSC 200 at various scanning rates from 10 to 1 K min^{-1} under dry nitrogen gas flow. The transition temperature and enthalpy were evaluated by extrapolating to zero heating rates. Indium and tin were used as reference standards for temperature and enthalpy.

The simultaneous DSC-XRD instrument [7] was set on a Mac Science MXP18 SRA X-ray diffractometer (DSC-WAXRD) [8] operated at 40 kV and 300 mA. The wavelength of monochromatic X-ray was 0.1540 nm. The scintillation counter was scanned at 10° min^{-1} in the 2θ range from 4° to 8°, which corresponded to 1.1 nm$<s^{-1}=(2\sin\theta/\lambda)^{-1}<$2.2 nm with the space resolution of 10^{-4} nm. The XRD profile for the fiber and crystalline specimens were observed by an imaging plate detector DIP-2000.

For the small angle X-ray measurement, the DSC-XRD instrument was set on the small angle X-ray scattering optics (DSC-SRXRD) at BL-10C of Photon Factory, High Energy Accelerator Research Organization, Tsukuba, Japan. The wavelength of monochromatic X-ray for DSC-SRXRD was 0.1488 nm. The scattering X-ray was detected by a one-dimensional position sensitive proportional counter (PSPC). The distance between specimen and PSPC was 680 nm, which covered 1.25 nm$<s^{-1}=(2\sin\theta/\lambda)^{-1}<$200 nm. The simultaneous DSC-XRD measurement was carried out at 5 K min^{-1}, and XRD profiles were stored for each 2.0 K (DSC-SRXRD) and 2.5 K (DSC-WAXRD), respectively. The temperature and enthalpy were calibrated by pure indium and tin.

Results and discussion

DSC curves of poly(oxyhexamethyleneoxy-2,7-phenanthrenedicarbonyl) (PPE*n*6) with various thermal history are shown in Fig. 1. The heating curve *a* for the precipitated powder on heating of PPE*n*6 shows two endothermic peaks at around 220 and 240°C. The cooling curve *b* from the molten state shows one exothermic peak at 228°C. The curve *c*, obtained by heating immediately after cooling from the molten state to 205°C, shows two endothermic peaks at 230 and 245°C. The cooling curve *d* from the molten state to 100°C shows two exothermic peaks at 228 and 195°C. From the optical microscopic observation, the clear domain boundary and the focal conic texture indicated.

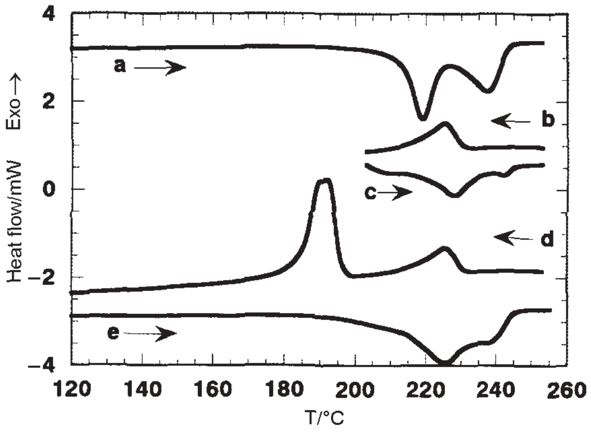

Fig. 1 DSC curves of PPE*n*6 with various thermal histories measured at 2 K min^{-1}

The existence of smectic phase between two exothermic peaks on cooling. However, the temperature range between two endothermic peaks on heating was too narrow to determine the structure. DSC curves of PPE*n*8 showed almost the same tendency with PPE*n*6.

The transition temperature and enthalpy of PPE*n*6 on cooling were obtained by extrapolating the initial temperature of transitions to zero scanning rate as shown in Fig. 2. The obtained transition temperature and enthalpy for PPE*n*6, *n*7 [3] and *n*8 were listed in Table 1. The equilibrium thermodynamic quantities are: $T_{\mathrm{L\text{-}S}}$=230.5°C, $\Delta H_{\mathrm{L\text{-}S}}$=4.5 kJ mol^{-1} (molar enthalpy was evaluated for repeating unit) for the transition from the isotropic liquid to the smectic phase, and $T_{\mathrm{S\text{-}C}}$=200.2°C, $\Delta H_{\mathrm{S\text{-}C}}$= 9.0 kJ mol^{-1} for the smectic phase to the crystalline phase for PPE*n*6. The transition entropy from the isotropic liquid to the smectic phase of PPE*n*6 ($\Delta S_{\mathrm{L\text{-}S}}$) and PPE*n*8 were 9.0 and 9.6 J mol^{-1} K^{-1}, respectively. These $\Delta S_{\mathrm{L\text{-}S}}$ were almost double of the transition entropy (4.5 J mol^{-1} K^{-1}) [5] reported for the polyesters containing biphenyl moieties as a mesogen unit in the main chain, which formed the smectic phase for odd

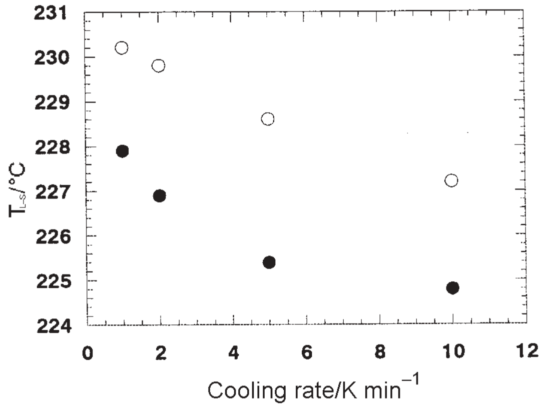

Fig. 2 Relationship between the cooling rate and transition temperatures; ○ – the initial transition temperature; ● – the transition peak temperature

methylene carbon number family and the nematic phase for even carbon number on cooling. The larger ΔS_{L-S} value of PPE*n*6 is due to the strong interaction between phenanthrene moieties comparing with biphenyl moieties.

Table 1 Transition temperature and enthalpy obtained by extrapolation to zero cooling rate

	I to S_A		S_A to S_C		S_X to *C*	
	T/°C	Δ*H*/kJ mol^{-1}	*T*/°C	Δ*H*/kJ mol^{-1}	*T*/°C	Δ*H*/kJ mol^{-1}
*n*6	230.5	4.5			200.2	9.0
*n*7	148.2	1.2	129.8	6.1	105.0	10.5
*n*8	195.3	4.5			189.1	9.2

Two-dimensional X-ray diffraction pattern of PPE*n*6 fiber is shown in Fig. 3 (A). The PPE*n*6 fiber was drawn at 210°C in the smectic A phase and quenched to room temperature. A couple of diffraction spot was observed in the parallel direction to the fiber axis. The spacing calculated from the diffraction was 1.98 nm, which was close to the calculated length of the extended length of repeating unit of PPE*n*6 assuming all *trans* conformation of alkyl chain. Therefore, the diffraction spot is assigned to the (001) diffraction of PPE*n*6 fiber. The fiber X-ray diffraction profile indicates that the extended PPE*n*6 molecules are oriented perpendicular to the smectic layer. Namely, this fiber diffraction pattern strongly suggests the smectic A structure of PPE*n*6 between 220 and 200°C on cooling. Figure 3 (B) is the X-ray diffraction pattern of the crystalline PPE*n*6 film prepared by cooling at 1 K min^{-1} from the molten state to room temperature. The (001) diffraction peak was also observed slightly in Fig. 3 (B). However, other diffraction peaks were found clearly in the crystalline state of PPE*n*6.

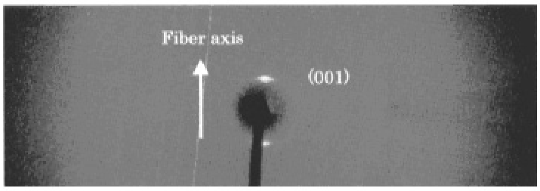

A

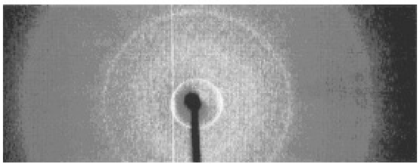

B

Fig. 3 A – Fiber X-ray diffraction profile of PPE*n*6 drawn at 210°C and B – X-ray diffraction profile of crystalline state of PPE*n*6

The relationship between the (001) spacing ($d_{(001)}$) evaluated from the X-ray diffraction of the crystalline state of PPEs and the methylene carbon number (n) is shown in Fig. 4. The linear relationship between $d_{(001)}$ and n indicates the same relation between the crystalline structure and molecular conformation for the PPEs with even methylene carbon number. The slope of this relationship gives the length of one methylene group, and also the value obtained by extrapolating this relationship to n=0 gives the length of main chain except alkyl chain, in other word, the length of mesogenic group. From the relationship between $d_{(001)}$ and n, the increase of length with methylene group and the length of mesogenic unit were 0.124 and 1.126 nm, respectively.

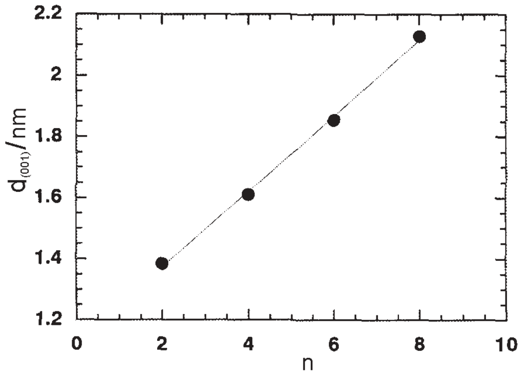

Fig. 4 Relationship between methylene carbon number (n) and (001) spacing ($d_{(001)}$) observed by X-ray diffraction profile of the crystalline phase for PPE at room temperature

From these results, the possible conformational model of PPEs with even methylene carbon number is shown in Fig. 5. The methylene groups are aligned to the *c*-axis of crystal, and the phenanthrene group exists obliquely with angle 30° to the *c*-axis. The molecular model shown in Fig. 5 is based on the molecular conformation in the smectic A phase.

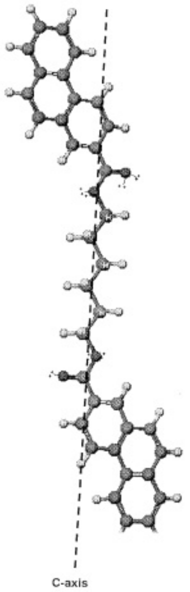

Fig. 5 Conformational model of PPEs with even methylene carbon number. Model shows PPE*n*6

The simultaneous DSC-SRXRD result of PPE*n*6 on cooling was shown in Fig. 6. PPE*n*6 was cooled from 275 to 160°C at 2 K min^{-1}. Two exothermic transitions were observed in DSC curve (A), the peak at 240 and 210°C are the isotropic–smectic transition and the crystallization, respectively. The temperature resolved XRD profiles changed at both transitions. The diffraction peak at 0.5 nm^{-1} ($s=2\sin\theta/\lambda$) appears at the isotropic–smectic transition and grow during the transition peak at around 240°C. Only one diffraction peak at 0.5 nm^{-1} was observed in the smectic A phase same as Fig. 3 (A). The sharp diffraction peak suggests that phenanthrene group stacks each other and forms regular spacing in the smectic A phase. This sharp diffraction peak changed to the broader one at the crystallization. During the crystallization, new diffraction peaks appeared at 0.3 and 0.62 nm^{-1}. The broad diffraction peaks at temperature below 200°C indicates the lower crystallinity of PPE*n*6. The diffraction peak from the smectic layer close to 0.02 nm^{-1} is hard to evaluate the maximum value (s_{max}). However, 2nd and 4th order diffraction peaks were observed at 0.15 and 0.3 nm^{-1}, respectively. The layer thickness calculated from these higher-order diffraction peaks is 13 nm, that is, five or six repeating units consist the layer.

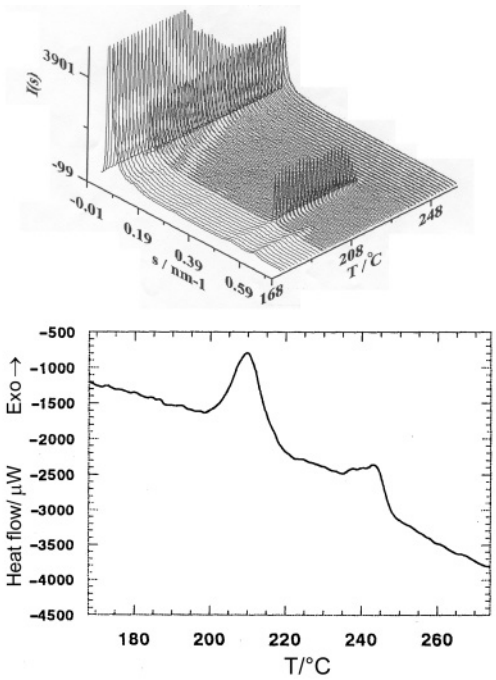

Fig. 6 Temperature resolved XRD profiles at various temperatures (upper) and DSC curve (lower) for PPE*n*6 observed by DSC-XRD at 2 K min^{-1} from the molten state to the crystal state

The temperature dependency of $d_{(001)}$ of PPE*n*6 observed by DSC-WAXRD is shown in Fig. 7. On heating, the $d_{(001)}$ increased linearly at temperature up to 170°C and increased rapidly at temperature above 180°C, at which the endothermic peak started. This diffraction peak disappeared at 230°C. On the other hand, the diffraction peak of s=0.51 nm^{-1} appeared at 225°C on cooling indicating the isotropic smectic transition. The $d_{(001)}$ decreases linearly with decreasing temperature from 225 to 205°C, which corre-

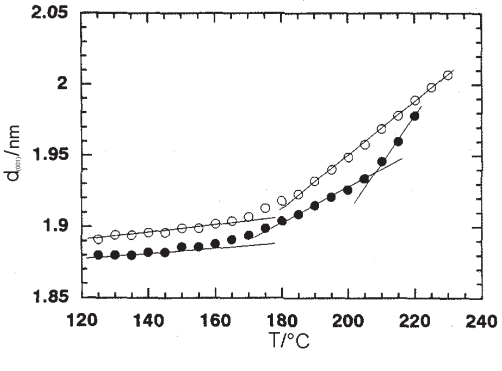

Fig. 7 ○ – temperature dependence of $d_{(001)}$ of PPE*n*6 on heating; ● – cooling observed by DSC-XRD at 2 K min^{-1}

sponds to the isotropic smectic transition region (DSC curve *d* in Fig. 1). The slope of $d_{(001)}$ changes slightly between 205 and 170°C, which closes to the crystallization. The $d_{(001)}$ decreases again linearly with decreasing temperature from 170 to 120°C.

The linear expansion coefficient of $d_{(001)}$ based on the $d_{(001)}$ value of the crystalline state at room temperature, 1.88 nm, was evaluated from Fig. 6. The linear expansion coefficient was obtained as follows;

Heating: $1.5\cdot10^{-4}$ K^{-1} (120–165°C), and $1.0\cdot10^{-3}$ K^{-1} (165–230°C)

Cooling: $1.3\cdot10^{-4}$ K^{-1} (120–160°C), $5.7\cdot10^{-4}$ K^{-1} (165–200°C) and $1.7\cdot10^{-3}$ K^{-1} (205–220°C)

The linear expansion coefficient of $d_{(001)}$ in the crystalline state is almost the same on heating and cooling. Comparing with the data of PPEs of odd *n* number, the linear expansion coefficient of $d_{(001)}$ in the crystalline state of PPE*n*6 is smaller than that of PPE*n*7 due to the conformational difference. The mesogenic group of PPE with even *n* number was expected to tilt with angle 30° to the *c*-axis, as described above. However, the mesogen group of PPE with odd number family is thought to be parallel to the *c*-axis [3, 9]. The linear expansion coefficients of *d*(001) for PPE*n*6, *n*7 [3] and *n*8 observed during both heating and cooling are listed in Table 2.

Table 2 Thermal expansion coefficient of the $d_{(001)}$ spacing

		Crystalline phase/ K^{-1}	Transition region/ K^{-1}	S_C phase/ K^{-1}	S_A phase/ K^{-1}
*n*6	Heating	$1.5\cdot10^{-4}$ (120–165°C)	$1.0\cdot10^{-3}$ (165–230°C)		
	Cooling	$1.3\cdot10^{-4}$ (120–160°C)	$5.7\cdot10^{-4}$ (165–200°C)		$1.7\cdot10^{-3}$ (205–220°C)
*n*7	Heating	$2.3\cdot10^{-4}$ (30–110°C)	$4.7\cdot10^{-4}$ (115–150°C)		$2.1\cdot10^{-3}$ (150–165°C)
	Cooling	$2.9\cdot10^{-4}$ (30–90°C)		$1.7\cdot10^{-3}$ (100–120°C)	$1.7\cdot10^{-3}$ (120–100°C)
*n*8	Heating	$1.2\cdot10^{-4}$ (90–150°C)	$1.0\cdot10^{-3}$ (190–200°C)		
	Cooling	$1.2\cdot10^{-4}$ (90–130°C)			$1.5\cdot10^{-3}$ (190–195°C)

The linear expansion coefficients of $d_{(001)}$ in the smectic A phase of PPE*n*6 and PPE*n*7 are almost the same ($1.5\cdot10^{-3}$ K^{-1} for PPE*n*7) [3]. However, linear expansion coefficients of $d_{(001)}$ observed during melting on heating ($1.0\cdot10^{-3}$ K^{-1}) was about a half of that obtained in the smectic phase on cooling ($1.7\cdot10^{-3}$ K^{-1}), and was about double of that observed during the crystallization on cooling ($5.7\cdot10^{-4}$ K^{-1}). As expected from the (001) diffraction peak in the smectic phase and the crystalline phase shown in Fig. 6, the crystalline structure of PPE*n*6 was based on the molecular conformation and alignment of the smectic A phase. These facts suggest that the smectic phase coexist with the crystal phase on heating in the temperature region between two endothermic peaks.

References

1 H. Yoshida, K. Masaka and S. Nakamura, Reports on Progress in Polymer Physics in Japan, 41 (1998) 211.
2 H. Yoshida, M. Honma, K. Masaka and S. Nakamura, Photon Factory Activity Report, 16 (1998) 117.
3 H. Yoshida, Y. Houshito, K. Mashiko, K. Masaka and S. Nakamura, J. Therm. Anal. Cal., 60 (2001) 453.
4 J. Watanabe and M. Hayashi, Macromolecules, 22 (1989) 4083.
5 W. R. Krigbaum, J. Watanabe and T. Ishikawa, Macromolecules, 16 (1983) 1271.
6 H. Sackmann and D. Demus, Mol. Cryst. Liq. Crys., 21 (1973) 239.
7 H. Yoshida, R. Kinoshita and Y. Teramoto, Thermochim. Acta, 264 (1995) 173.
8 H. Yoshida, Thermochim. Acta, 267 (1995) 239.
9 H. Yoshida, K. Mashiko, K. Masaka and S. Nakamura, unpublished data.